# Hadron production and bottomia suppression at the LHC

Georg Wolschin

Heidelberg University

Institut für Theoretische Physik

Philosophenweg 16

D-69120 Heidelberg


MPIK_19.01.2015

# Topics

1. Introduction: Relativistic heavy ions @ LHC
2. Stopping
3. Particle production: Relativistic Diffusion Model (RDM)
4. Bottomium suppression in the Quark-Gluon Plasma (QGP)
5. Conclusion

# 1. Introduction

## LHC detectors: ATLAS, CMS, LHCb, ALICE

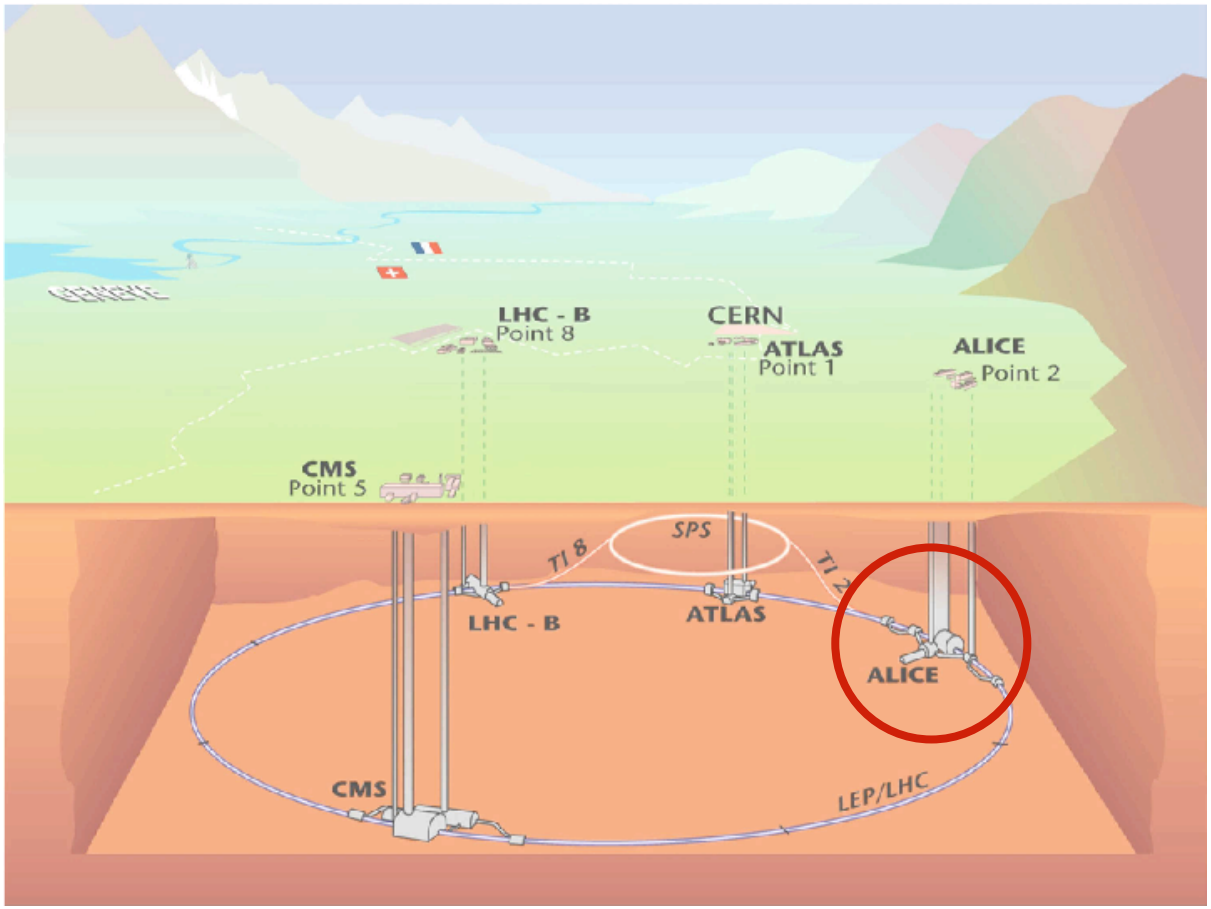


**p+p: 7,8,13,(14) TeV**

**Pb+Pb:**

1st lead beam Nov 6, 2010
**@ 2.76 TeV 2011/12**

- PbPb @ 5.125 TeV
  ≈ Oct. 2015
  (design energy 5.52 TeV)

- pPb @ 5.02 TeV 2012/13

# ATLAS, CMS in pp @ 7/8 TeV: Higgs boson discovery

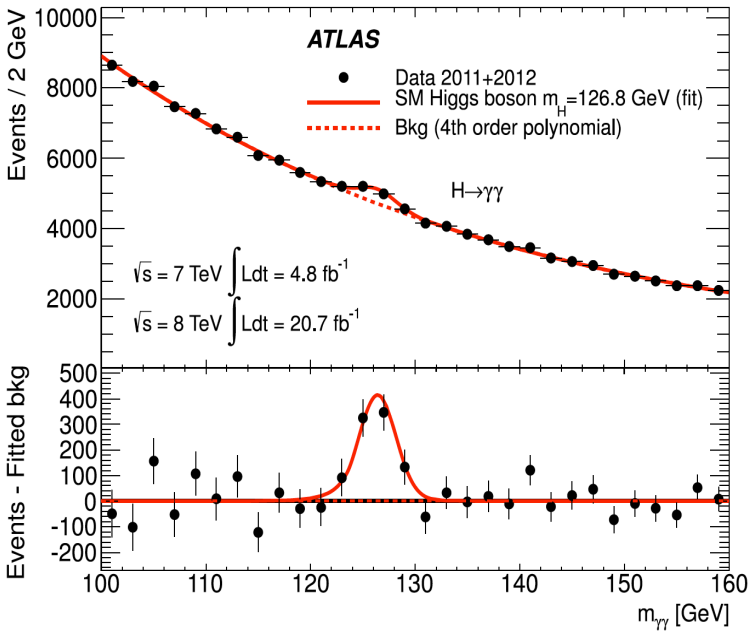


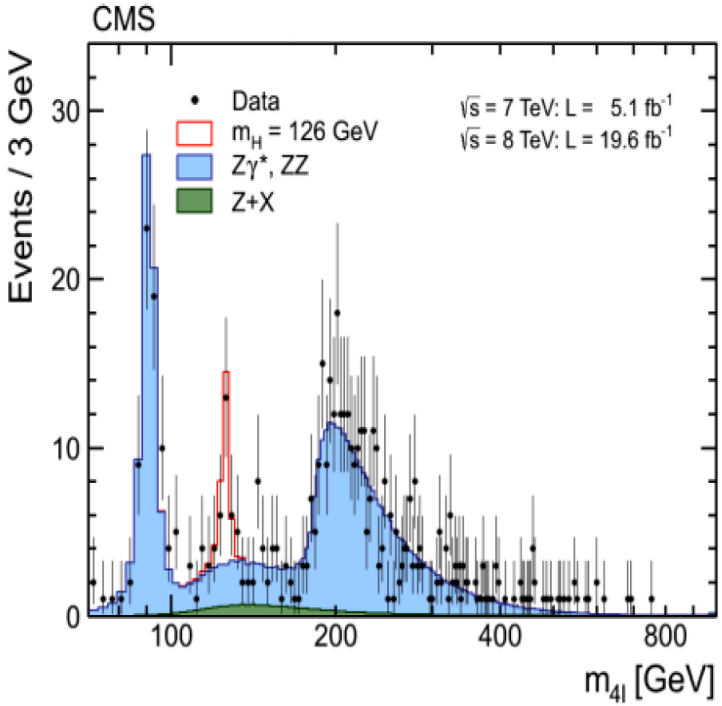


ATLAS, Two-gamma channel. Combined channels:
$m_H$ = 126.0 +/- 0.4(stat) +/- 0.4(sys) GeV
Phys.Lett. B716, 1 (2012).

CMS, Four-lepton channel. Combined:
$m_H$ = 125.3 +/- 0.4(stat) +/- 0.5(sys) GeV
Phys.Lett. B716, 30 (2012).

# LHC Detectors
## for Relativistic Heavy-Ion physics

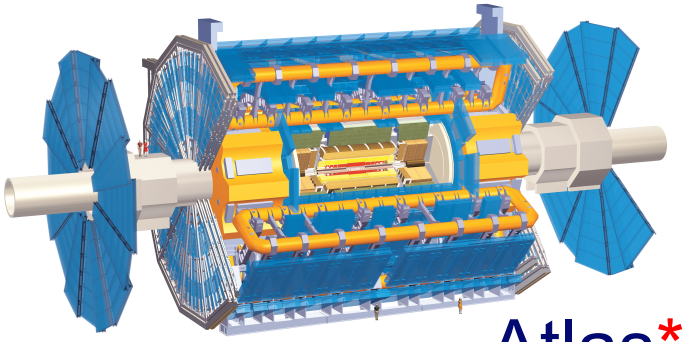

Atlas*

**≈ 50 HI people**

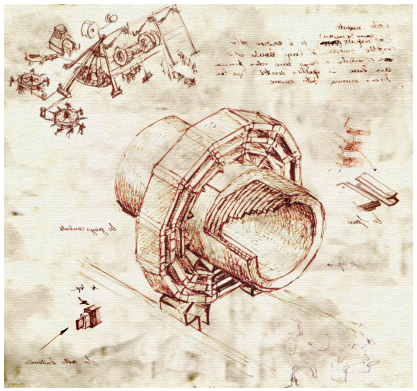

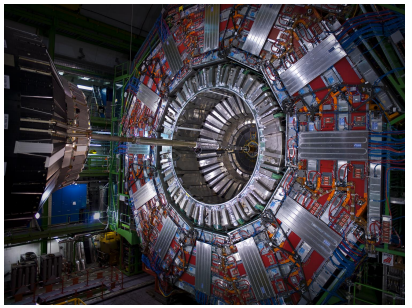

CMS*

da Vinci style

**≈ 60 HI people**

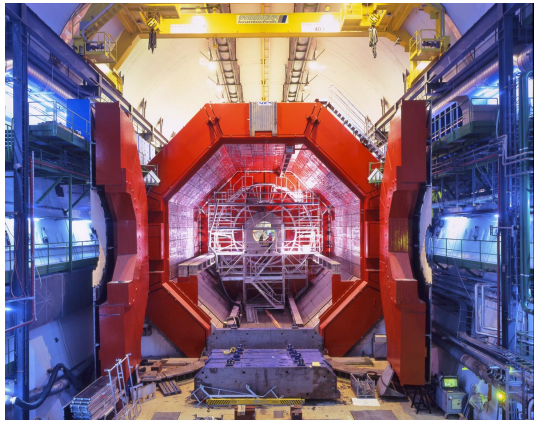

Alice*: L3 magnet

**≈ 1,000 HI people**

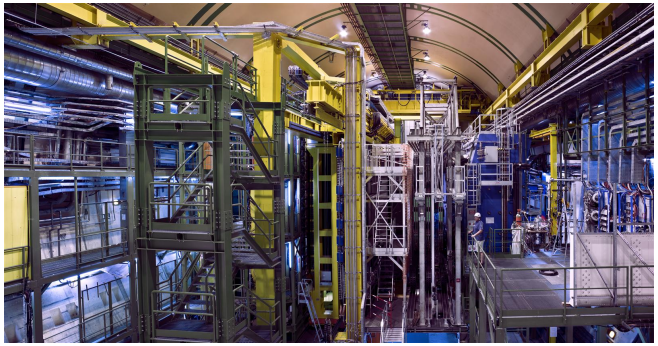

LHCb

**p-Pb only**

* heavy-ion capability

# 2. Stopping: Net protons/baryons and gluon saturation

Stopping occurs mainly through the interaction of valence quarks with gluons

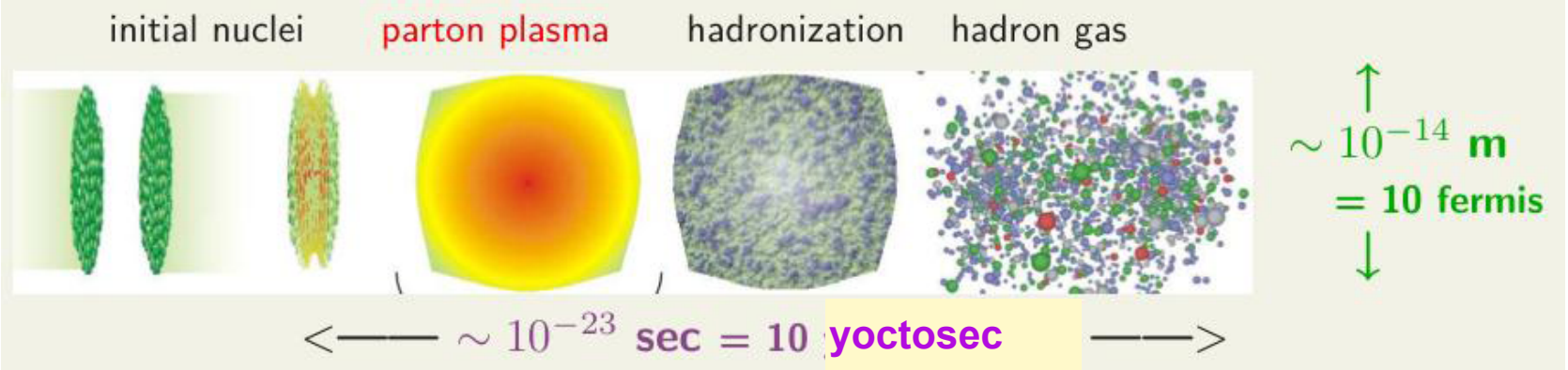


Artwork: Nikhef/S.Bass

At RHIC (≤ 0.2 TeV) and LHC (≤ 5.52 TeV) energies, initially a state of very high gluon density is formed, which transforms into a strongly coupled quark-gluon plasma, and then hadronizes after ≈$10^{-23}$ s into mesons and baryons.

Search for signatures of the QGP, and the initial Gluon Condensate

# QCD

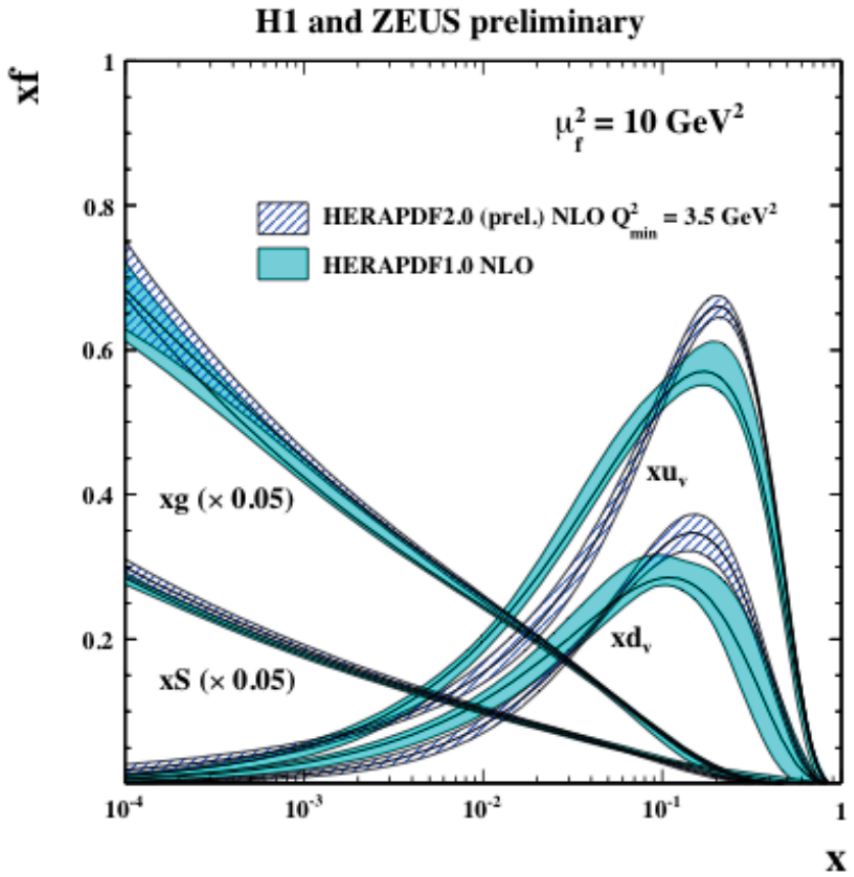


Structure functions (pdfs) from e + p deep inelastic scattering (DIS) at HERA (DESY) (from H. Abramowicz, ICNFP2014)

x: longitudinal momentum fraction carried by the parton

- Gluon structure functions grow with increasing $Q^2$ and 1/x
- At small x and high energy, gluons dominate the dynamics.
- The gluon distribution should saturate at very small x. The saturation scale is $Q_s^2(x) \sim A^{1/3} x^{-\lambda}, \lambda \sim 0.3$

→ Saturation effects expected to be more pronounced in nuclei

# Microscopic formulation of stopping/baryon transport for RHIC, LHC physics

- The net-baryon transport occurs through valence quarks:
- Fast valence quarks in one nucleus scatter in the other nucleus by exchanging soft gluons, and are redistributed in rapidity space.
- The valence quark parton distribution is well known at large x, which corresponds to the forward (and backward) rapidity region, and it can be used to access the small-x gluon distribution in the target.

**Y. Mehtar-Tani and GW, Europhys. Lett. 94, 62003 (2011)**
**Phys. Lett. B688, 174 (2010)**
**Phys. Rev. C80, 054905 (2009)**
**Phys. Rev. Lett. 102,182301 (2009)**

**GW, Prog. Part. Nucl. Phys. 59, 374 (2007)**
**Phys. Rev. C 69, 024906 (2004)**

The differential cross-section for valence quark production with rapidity y and transverse momentum $p_T$ in a high-energy heavy-ion collision is

$$\frac{dN}{d^2p_T dy} = \frac{1}{(2\pi)^2}\frac{1}{p_T^2}\, x_1 q_v(x_1, Q_f)\, \varphi\,(x_2, p_T)$$

The contribution of the valence quarks in the forward moving nucleus to the rapidity distribution of hadrons is then (integration over $p_T$):

$$\frac{dN}{dy} = \frac{C}{(2\pi)^2}\int \frac{d^2p_T}{p_T^2}\, x_1 q_v(x_1, Q_f)\, \varphi\,(x_2, p_T)$$

Valence quarks

Gluons

Where the transverse momentum transfer is $p_T$,

the longitudinal momentum fraction carried by the valence quark is $x_1 = p_T/\sqrt{s}\exp(y)$

and the soft gluon in the target carries $x_2 = p_T/\sqrt{s}\exp(-y)$.

# Stopping: Net-baryon rapidity distributions at SPS, RHIC, and LHC

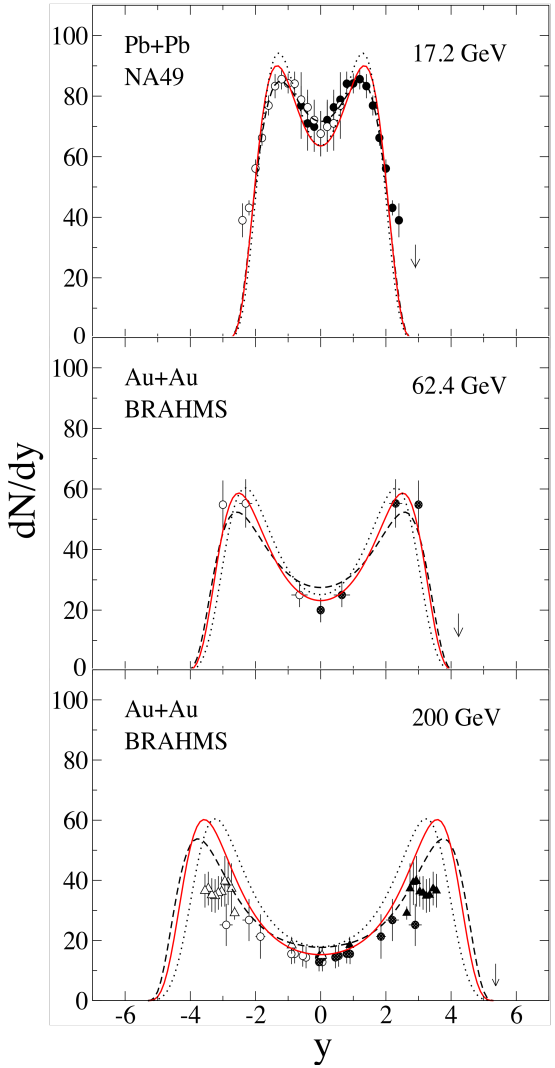


$$Q_s^2(x) \sim A^{1/3} x^{-\lambda}, \lambda \sim 0.3$$

- Central (0-5%) Pb+Pb (SPS) and Au+Au (RHIC) Collisions

- Dashed black curves: $Q_0^2$ = 0.08 GeV$^2$ , λ=0
  Solid red curves: $Q_0^2$ = 0.07 GeV$^2$, λ=0.15
  Dotted black curves: $Q_0^2$ = 0.06 GeV$^2$, λ=0.3

- A larger gluon saturation scale produces more baryon stopping, as does a larger value of A.

- The saturation scale is $Q_s^2(x) = A^{1/3} Q_0^2 x^{-\lambda}$

**Calculations are in a QCD-inspired model**

**Y. Mehtar-Tani and GW, Phys. Rev. Lett. 102,182301 (2009).**

# Net-baryon rapidity distributions at LHC: prediction

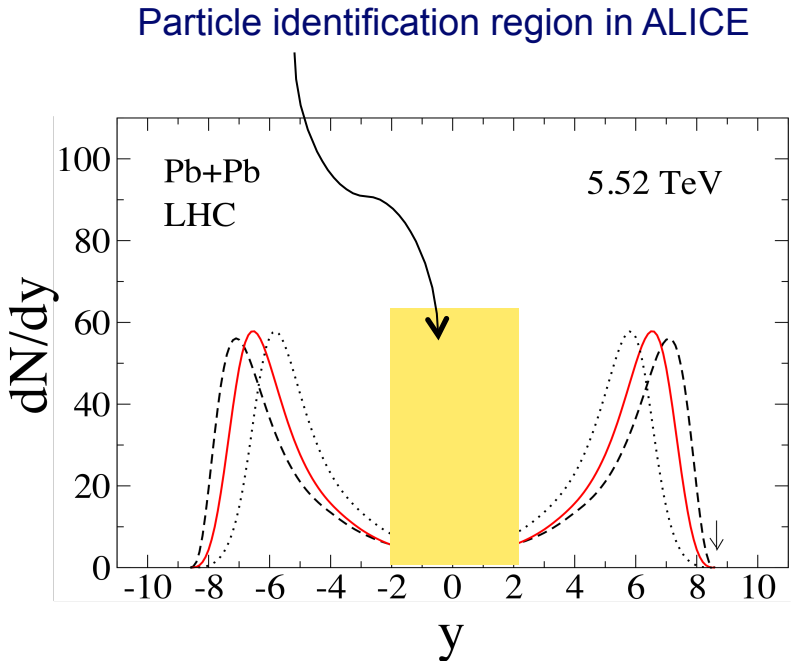


**Y. Mehtar-Tani and GW**
**Phys. Rev. Lett. 102,182301 (2009)**

- Central (0-5%) Pb+Pb collisions, $y_{beam} = 8.68$
- **A larger gluon saturation scale produces more baryon stopping; the fragmentation peak position is sensitive to** $\lambda$ (dashed $\lambda = 0$, solid $\lambda = 0.15$, dotted $\lambda = 0.3$)
- The midrapidity value of the net-baryon distribution is small, but finite: dN/dy (y = 0) ≈ 4. The **total yield** is normalized to the number of baryon participants, $N_B \approx 357$.

Measurements with particle identification will be confined to the yellow region for the next years.

The fragmentation peaks seen in stopping are also relevant for particle production, where a central gluonic source arises that cancels out in the net baryon case: 3 sources for produced hadrons.

# 3. Particle production: Relativistic Diffusion Model (RDM)

$$\frac{\partial}{\partial t}R(y,t) = -\frac{\partial}{\partial y}\Big[J(y)R(y,t)\Big] + D_y\frac{\partial^2}{\partial y^2}[R(y,t)]^{2-q}$$

R (y,t) Rapidity distribution function. The standard linear Fokker-Planck equation corresponds to q = 1, and a linear drift function. For the three components k = 1,2,3 of the rapidity distribution (fragmentation plus central sources),

$$\frac{\partial}{\partial t}R_k(y,t) = -\frac{1}{\tau_y}\frac{\partial}{\partial y}\Big[(y_{eq}-y)\cdot R_k(y,t)\Big] + D_y^k\frac{\partial^2}{\partial y^2}R_k(y,t)$$

Linear drift term with relaxation time $\tau_y$ Diffusion term, $D_y$=const.

Relaxation time and diffusion coefficient are related through a dissipation-fluctuation theorem. The broadening is enhanced due to collective expansion.

$$< y_{1,2}(t) >= y_{eq}[1-\exp(-t/\tau_y)] \mp y_{max}\exp(-t/\tau_y)$$ mean value

$$\sigma^2_{1,2,eq}(t) = D_y^{1,2,eq}\tau_y[1-\exp(-2t/\tau_y)]$$ variance

**Linear Model:** G. Wolschin, Eur. Phys. J. A5, 85 (1999); with 3 sources: Phys. Lett. B 569, 67 (2003); PLB 698, 411 (2011); M. Biyajima, M. Ide, M. Kaneyama, T. Mizoguchi, and N. Suzuki, Prog. Theor. Phys. Suppl. 153, 344 (2004)

Equilibrium value of the rapidity determined from energy and momentum conservation as

$$y_{eq}(b) = -0.5 \cdot \ln \frac{\langle m_1^T(b)\rangle \exp(y_{max}) + \langle m_2^T(b)\rangle \exp(-y_{max})}{\langle m_2^T(b)\rangle \exp(y_{max}) + \langle m_1^T(b)\rangle \exp(-y_{max})}$$

with transverse masses

$$\langle m_{1,2}^T(b)\rangle = \sqrt{m_{1,2}^2(b) + \langle p_T\rangle^2}$$

For large beam rapidities (LHC) this reduces to

$$y_{eq}(b) \simeq 0.5 \cdot \ln \frac{\langle m_2^T(b)\rangle}{\langle m_1^T(b)\rangle}$$

And the impact-parameter dependent numbers of participants can be determined from the geometric overlap, or the Glauber model.

# Diffusion of produced particles in η-space

Pseudorapidity distributions of produced particles are obtained through the Jacobian transformation

$$\frac{dN}{d\eta} = \frac{dN}{dy}\frac{dy}{d\eta} = \frac{p}{E}\frac{dN}{dy} \simeq J(\eta, \langle m \rangle / \langle p_T \rangle)\frac{dN}{dy}$$

$$J(\eta, \langle m \rangle / \langle p_T \rangle) = \cosh(\eta) \cdot [1 + (\langle m \rangle / \langle p_T \rangle)^2 + \sinh^2(\eta)]^{-1/2}.$$

**GW, J.Phys. G40, 045104 (2013)**
**D. Roehrscheid, GW, Phys. Rev. C86, 024902 (2012)**

with the rapidity distribution
in the three-sources model

$$\frac{dN_{ch}(y, t = \tau_{int})}{dy} = N^1_{ch} R_1(y, \tau_{int}) + N^2_{ch} R_2(y, \tau_{int}) + N^{eq}_{ch} R_{eq}(y, \tau_{int}).$$

and the rapidity

$$y = 0.5 \cdot \ln((E + p)/(E - p))$$

$$\eta = -\ln[\tan(\theta/2)]$$

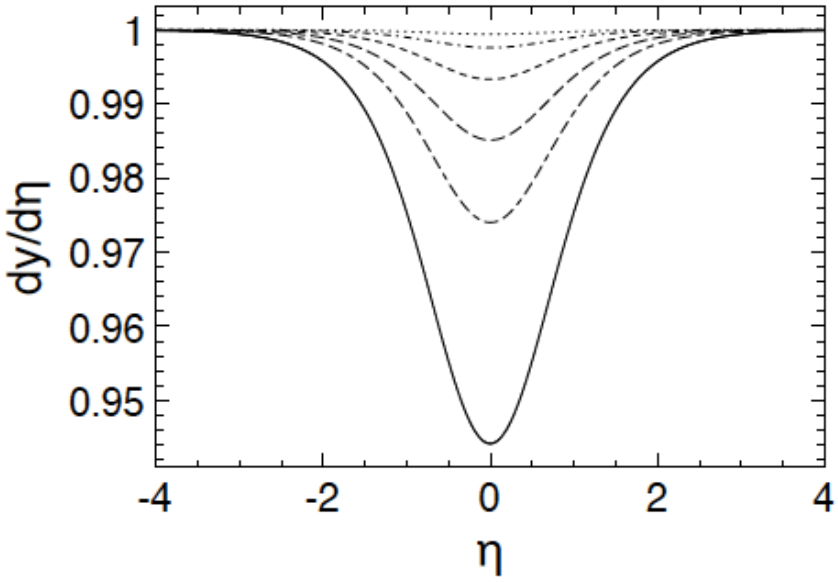


Figure 1: The Jacobian $dy/d\eta$ for $< m >= m_\pi$ and average transverse momenta (bottom to top) $< p_T >= 0.4, 0.6, 0.8, 1.2, 2$ and 4 GeV/c.

# Comparing data with the RDM calculation for produced charged hadrons

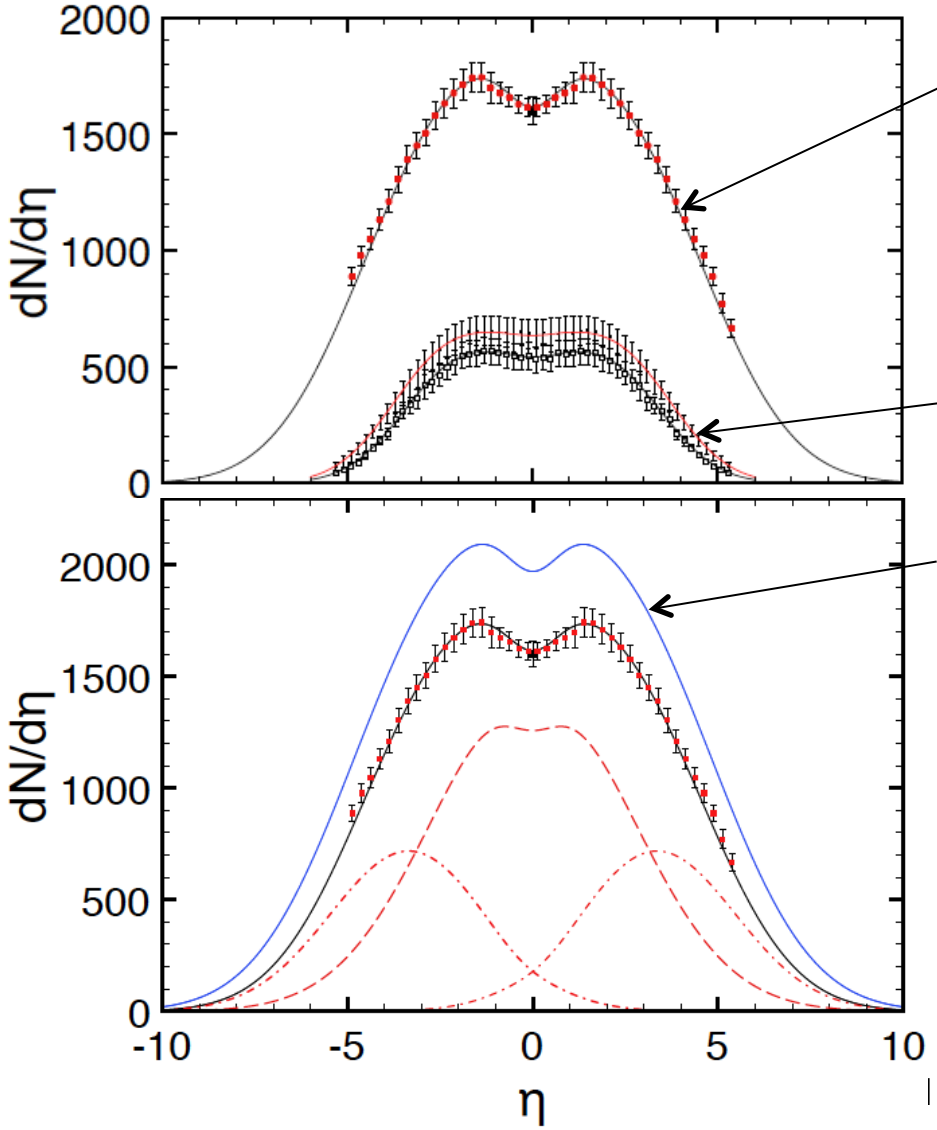


**Central PbPb @ 2.76 TeV**
(ALICE data; RDM calc.)

RHIC data
(PHOBOS)
130 and 200 GeV

**Prediction at 5.52 TeV**

**3 sources:** 2 symmetric fragmentation sources
1 midrapidity gluon-gluon source, modified by the Jacobian.

RDM parameters determined in $\chi^2$ minimizations

**GW, J. Phys. G40, 045104 (2013)**



[1] ALICE collab., PRL 105, 252301 (2010)
[2] ALICE collab., PRL 106, 032301 (2011)
[3] B.B. Back et al.,PHOBOS coll., PRL 87, 102303 (2001); PRL 91, 052303 (2003); PRC 83, 024913 (2011)

# Parameters of the 3-sources RDM at RHIC and LHC energies

**Table 1.** Three-sources RDM-parameters $\tau_{\rm int}/\tau_y$, $\Gamma_{1,2}$, $\Gamma_{\rm gg}$, and $N_{\rm gg}$. $N_{\rm ch}^{1+2}$ is the total charged-particle number in the fragmentation sources, $N_{\rm gg}$ the number of charged particles produced in the central source. Results for $\langle y_{1,2}\rangle$ are calculated from $y_{\rm beam}$ and $\tau_{\rm int}/\tau_y$. Values are shown for 0–5% PbPb at LHC energies of 2.76 and 5.52 TeV in the lower two lines, with results at 2.76 TeV from a $\chi^2$-minimization with respect to the preliminary ALICE data [2], and using limited fragmentation as constraint. Corresponding parameters for 0–6% AuAu at RHIC energies are given for comparison in the upper four lines based on PHOBOS results [1]. Parameters at 5.52 TeV denoted by * are extrapolated. Experimental midrapidity values (last column) are from PHOBOS [1] for $|\eta| < 1$, 0–6% at RHIC energies and from ALICE [13] for $|\eta| < 0.5$, 0–5% at 2.76 TeV.

| $\sqrt{s_{NN}}$ (TeV) | $y_{\rm beam}$ | $\tau_{\rm int}/\tau_y$ | $\langle y_{1,2}\rangle$ | $\Gamma_{1,2}$ | $\Gamma_{\rm gg}$ | $N_{\rm ch}^{1+2}$ | $N_{\rm gg}$ | $\frac{dN}{d\eta}\vert_{\eta\simeq 0}$ |
|---|---|---|---|---|---|---|---|---|
| 0.019 | $\mp$3.04 | 0.97 | $\mp$1.16 | 2.83 | 0 | 1704 | – | $314 \pm 23$ [1] |
| 0.062 | $\mp$4.20 | 0.89 | $\mp$1.72 | 3.24 | 2.05 | 2793 | 210 | $463 \pm 34$ [1] |
| 0.13 | $\mp$4.93 | 0.89 | $\mp$2.02 | 3.43 | 2.46 | 3826 | 572 | $579 \pm 23$ [1] |
| 0.20 | $\mp$5.36 | 0.82 | $\mp$2.40 | 3.48 | 3.28 | 3933 | 1382 | $655 \pm 49$ [1] |
| 2.76 | $\mp$7.99 | 0.87 | $\mp$3.34 | 4.99 | 6.24 | 7624 | 9703 | $1601 \pm 60$ [13] |
| 5.52 | $\mp$8.68 | 0.85* | $\mp$3.70 | 5.16* | 7.21* | 8889* | 13903* | 1940* |

# RDM $\chi^2$ fits to LHC/ALICE results for 2.76 TeV PbPb

GW, J. Phys. G40, 045104 (2013)

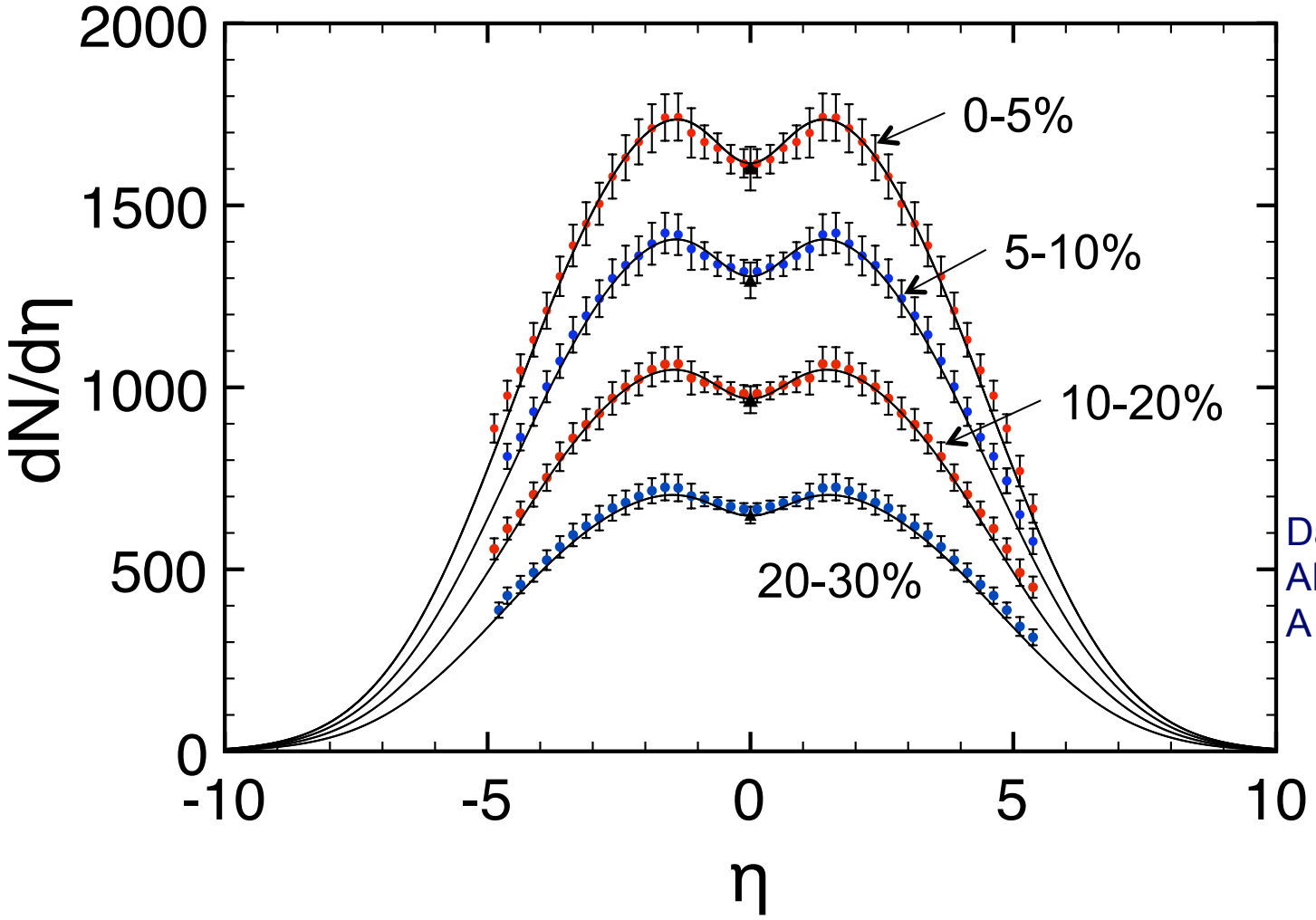


Data: M. Guilbaud et al., ALICE Coll., Nucl. Phys. A 904-905, 381c (2013)

# 3 sources, and prediction for 5.52 TeV PbPb

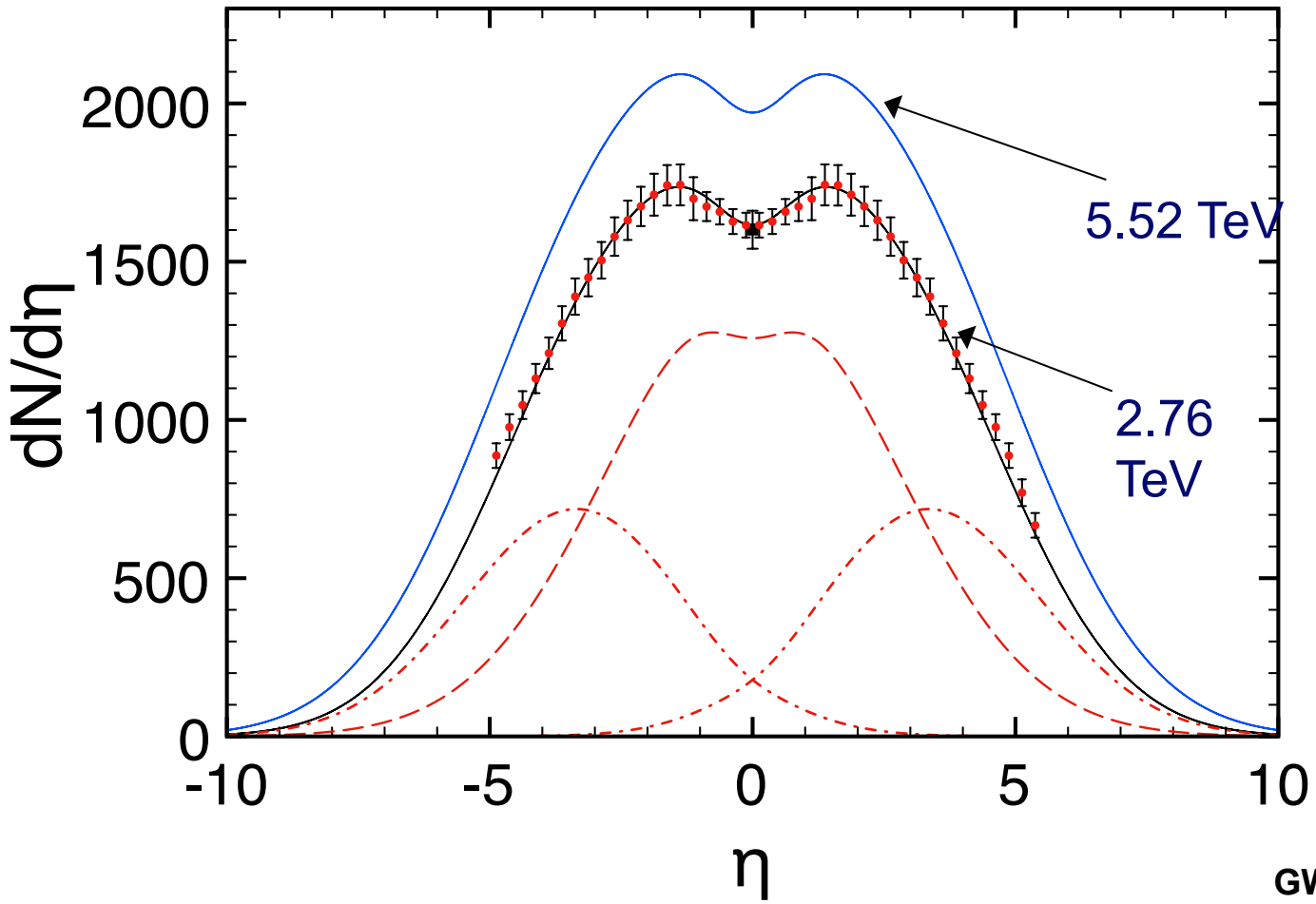


Centrality 0-5%

ALICE data

**GW, J. Phys. G40, 045104 (2013)**

# Content of the sources as function of energy

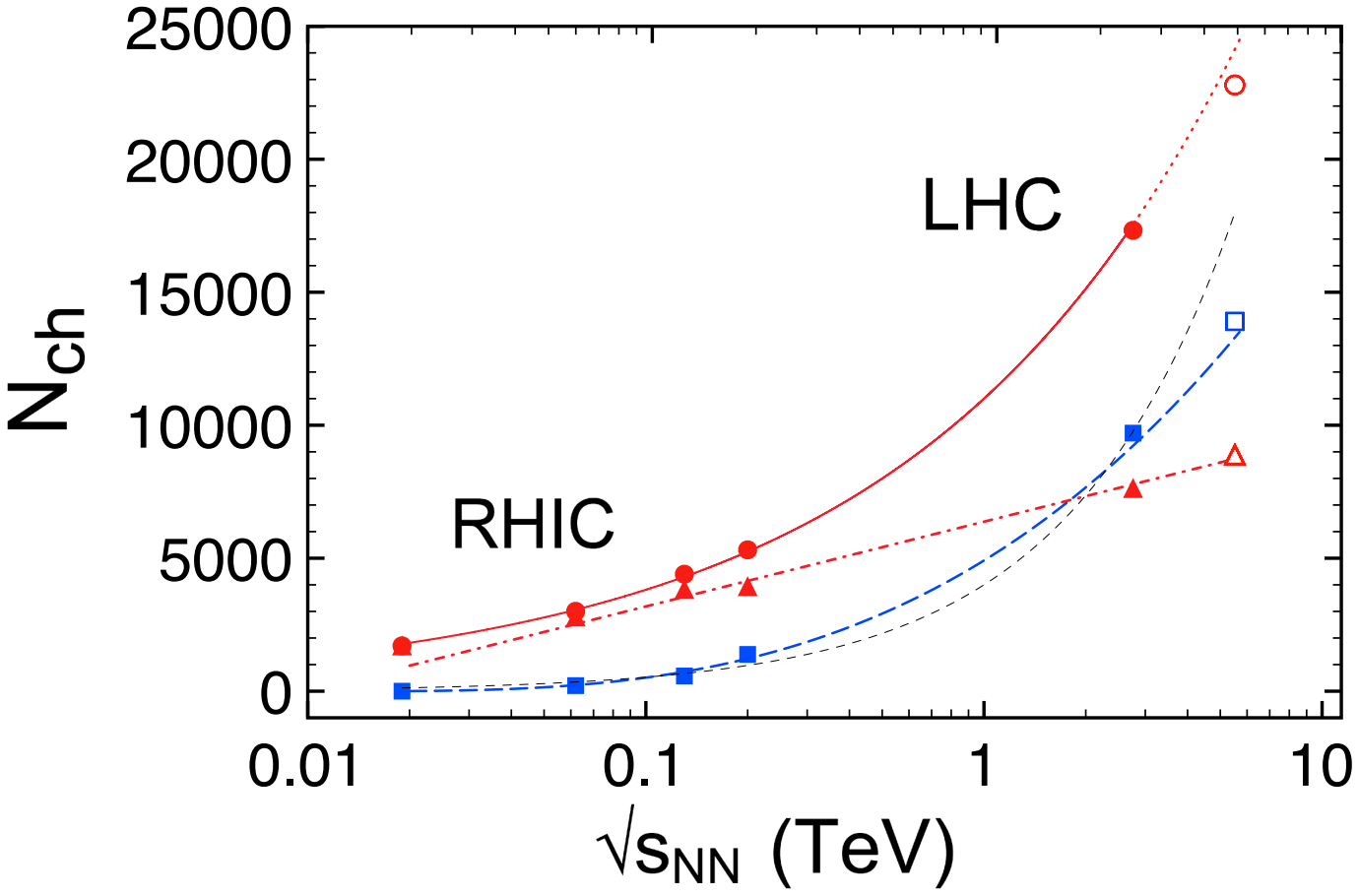


Centrality 0-5%

(RHIC 0-6%)

Fragmentation sources

$$\propto \ln(s_{NN}/s_0)$$

Central source

$$\propto \ln^3(s_{NN}/s_0)$$

[power law: ≈ $(s_{NN}/s_0)^{0.44}$]

**GW arXiv:1501.03026 (2015); PRC, in press**

# Content of the sources as function of energy

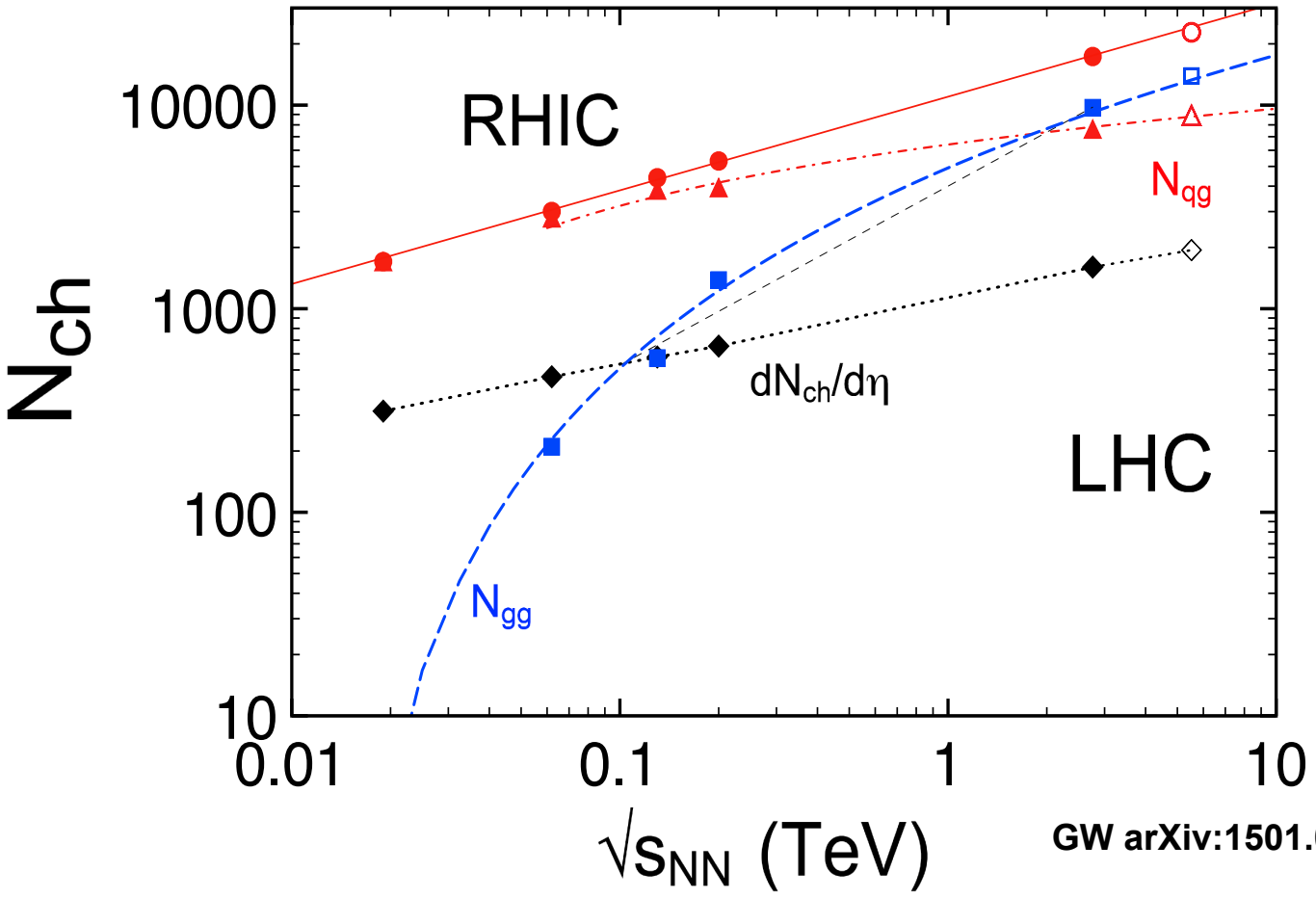


Centrality 0-5%

(RHIC 0-6%)

Fragmentation sources

$$\propto \ln(s_{NN}/s_0)$$

Central source

$$\propto \ln^3(s_{NN}/s_0)$$

**GW arXiv:1501.03026 (2015); PRC, in press**

# No midrapidity source below $E_{cm} \approx 20$ GeV

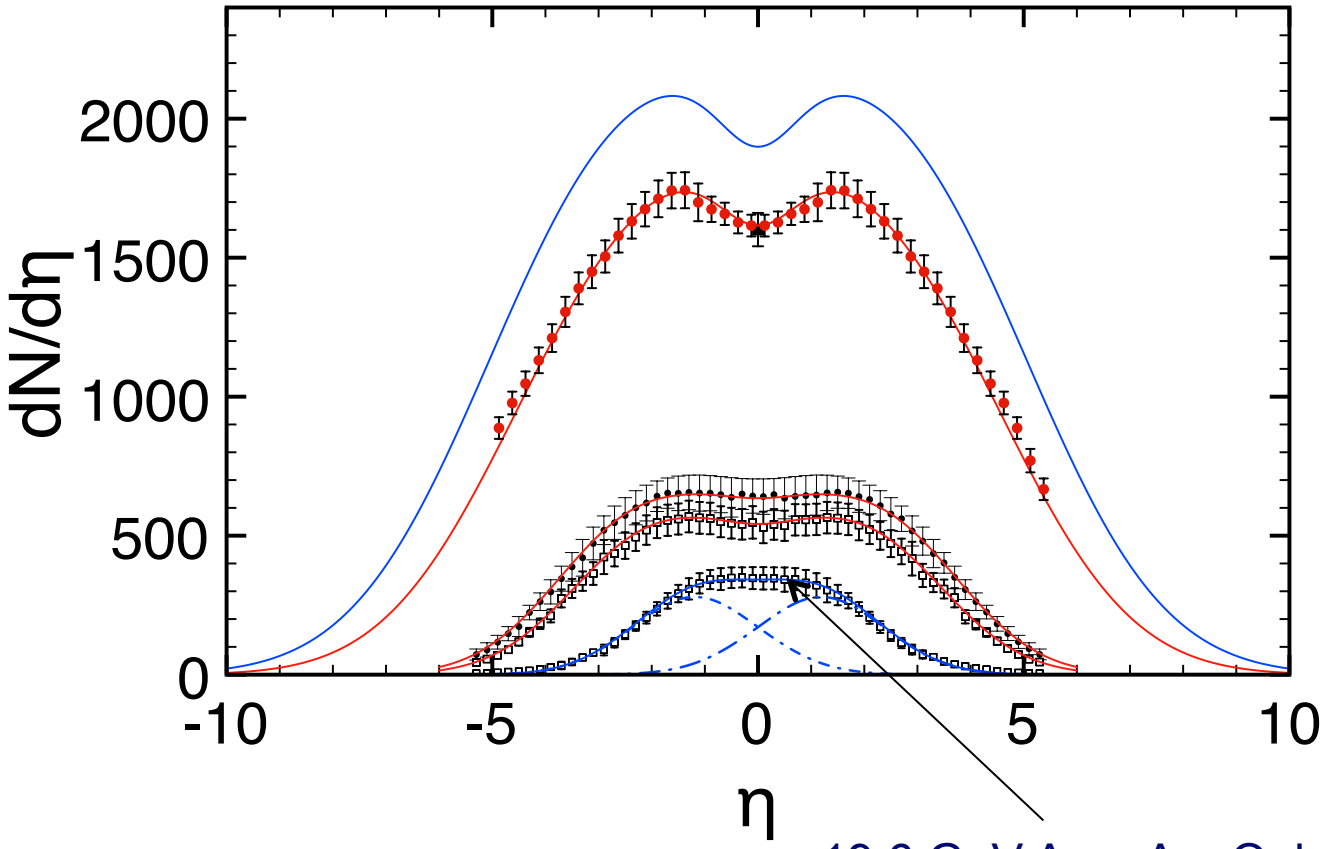


Centrality 0-5%

(RHIC 0-6%)

Fragmentation sources

$\propto \ln(s_{NN}/s_0)$

Central source

$\propto \ln^3(s_{NN}/s_0)$

19.6 GeV Au + Au: Only fragmentation sources

# Content of the central source as function of energy

Rise of the cross section with energy in the central distribution is driven by the growth of the gluon density at small *x*, but is "..suppressed by the quantum-classical interaction from the dense medium"

$$\frac{dN}{d\eta}|^{gg}_{\eta\simeq 0} \propto \ln^2(s_{NN}/s_0)$$

cf. M.F. Cheung and C.B. Chiu, arXiv:1111.6957; analogous to Froissart bound of the total cross section (approximate solution to leading order)

Total particle content in the *gg*-source by integrating over $\eta$:

$$\int_{-y_{\rm beam}}^{y_{\rm beam}} \frac{dN}{d\eta}|^{gg}_{\eta\simeq 0} d\eta \propto \ln^3(s_{NN}/s_0) \qquad \text{since} \qquad y_{\rm beam} = \ln(\sqrt{s_{NN}}/m_p)$$

$$\rightarrow N^{gg}_{tot} \propto \ln^3(s_{NN}/s_0)$$

as inferred from the phenomenological analysis: Room for further theoretical development.

# Asymmetric system: *p*Pb @ 5.02 TeV

- Asymmetric central and fragmentation sources for particle production

Min. bias 5.02 TeV pPb @ LHC

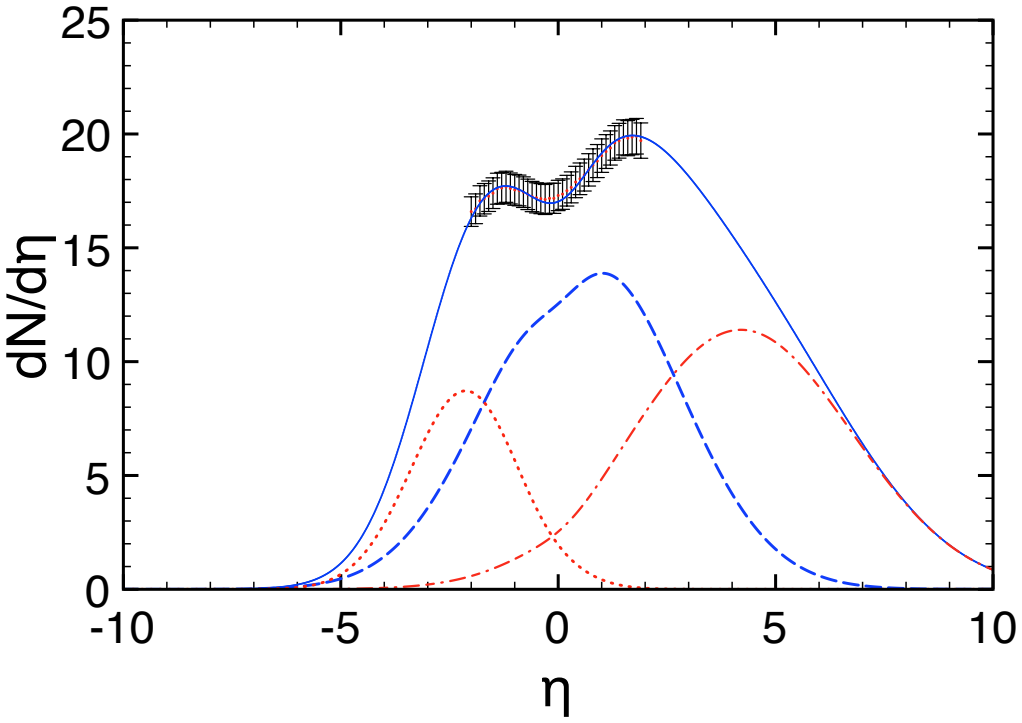


$p_p$= 4 TeV/c

$$\sqrt{s_{NN}} = \sqrt{\frac{Z_1 * Z_2}{(A_1 * A_2)}} * 2p_p = 5.02\mathrm{TeV}$$

$$y^{cm}_{\mathrm{beam}} = \mp \ln(\sqrt{s_{NN}}/m_0) = \mp 8.586$$

Calculation: GW, J. Phys. G40, 045104 (2013)

Midrap. data: ALICE collab., PRL 110, 032301 (2013)

# 3-sources model (RDM): *p*Pb @ 5.02 TeV

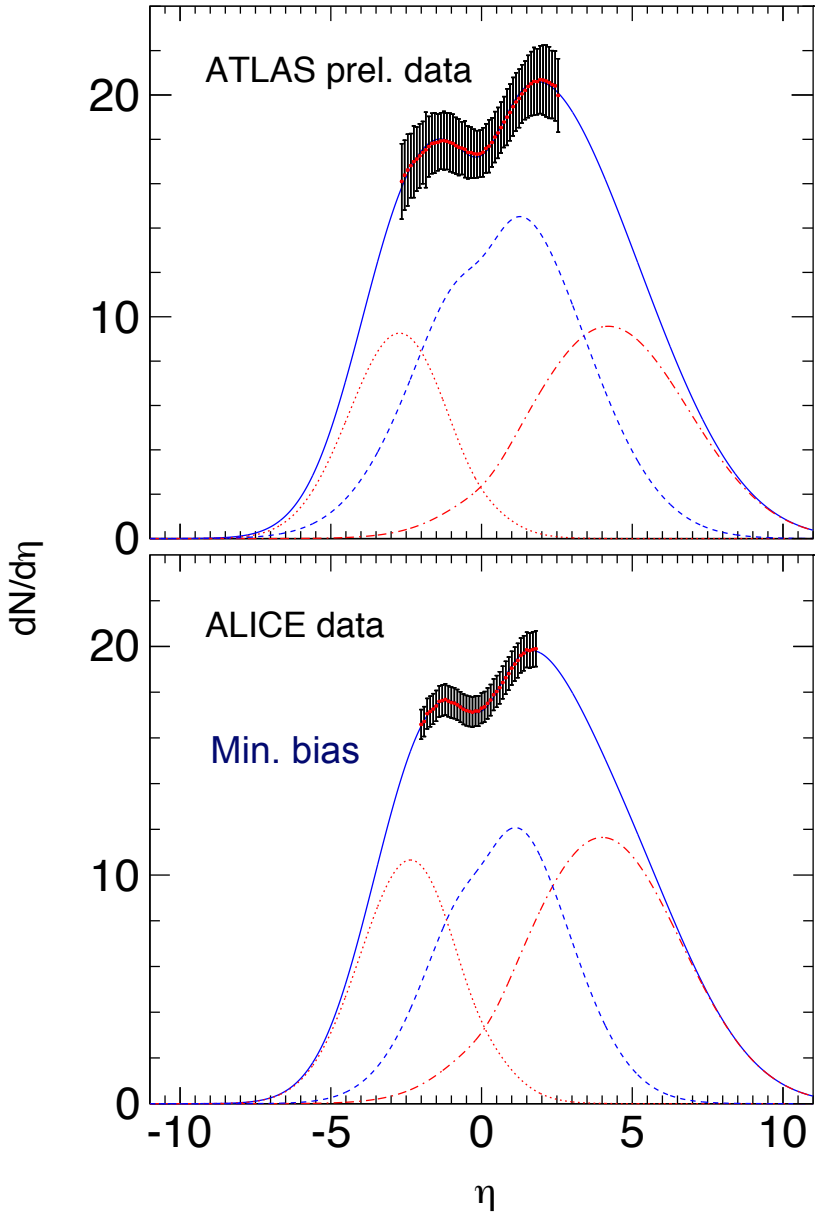


## Minimum bias charged hadrons in pPb

- ALICE 0-100% min. bias data and preliminary ATLAS 0-90% data are fully consistent once the latter are rescaled with the cross section ratio $\sigma$(0-90%)/$\sigma$(0-100%) = 0.898.
- The ≈ midrapidity gluon-gluon source is the largest particle production source. It is significantly modified by the Jacobian, whereas the fragmentation sources are almost gaussian.
- Data at larger values of $\eta$ needed to determine the particle content more precisely

Midrap. data: ALICE collab., PRL 110, 032301 (2013); 0-100% centrality

ATLAS prelim. data 0-90% scaled with the cross section ratio (90%/100%): ATLAS-CONF-2013-096 (2013)

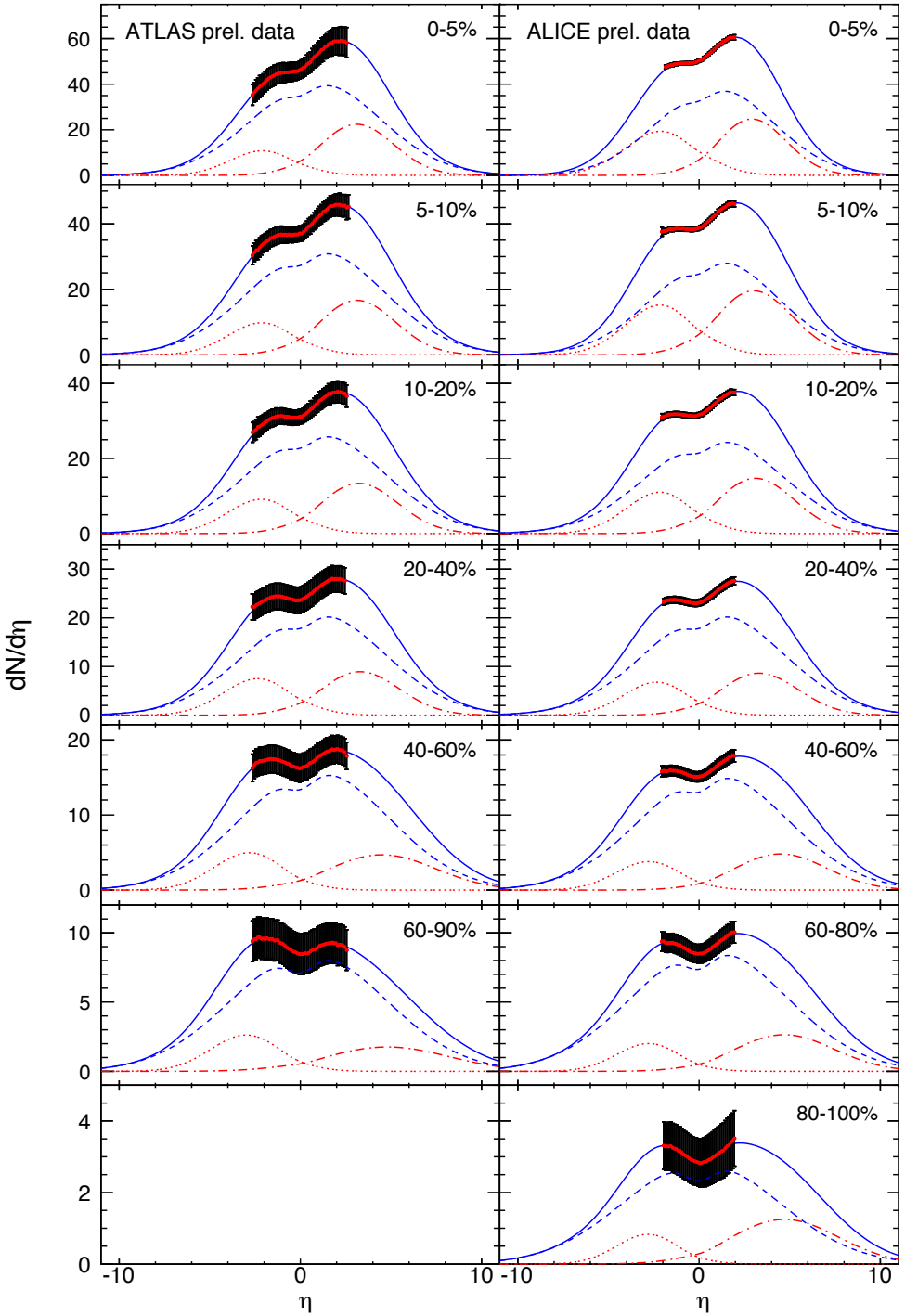


# Centrality dependence *p*Pb @ 5.02 TeV

- Good agreement of preliminary ATLAS and prel. ALICE results for most centralities
- The midrapidity gluon-gluon source remains the largest hadron production source at all centralities, the *p*-like source the smallest
- ( dN/dη)_max decreases from ≈ 60 at 0-5 % to ≈ 3 at 80-100 %

Calculations: P. Schulz and GW (2014)
$\chi^2$- minimizations with respect to the prel. data.

Preliminary data: A. Toia (ALICE collab./ CL1), Quark Matter Conf., Darmstadt (2014), Nucl. Phys. A931, 315 (2014); ATLAS-CONF-2013-096 (2013).

# Centrality dependence of the RDM-parameters in *p*Pb @ 5.02 TeV

**Table 1.** RDM parameters (mean values $< y_{1,2} >$ and widths $\Gamma_i$), and particle content of the sources for centrality-dependent *p*Pb collisions at 5.02 TeV. This $\chi^2$-optimization (per numbers of degrees of freedom, dof) uses ROOT [9], preliminary ALICE charged-hadron $dN/d\eta$ data [5], and equilibrium values $y_{eq}$ of the mid-rapidity source. The mean transverse momenta $\langle p_T \rangle$ are taken from [10]. The beam rapidity is $y_{beam} = \mp y_{max} = \mp 8.586$.

| centrality (%) | $\langle p_T \rangle$ GeV/$c$ | $y_{eq}$ | $\langle y_1 \rangle$ | $\langle y_2 \rangle$ | $\Gamma_1$ | $\Gamma_2$ | $\Gamma_{gg}$ | $N_1$ | $N_2$ | $N_{gg}$ | $\chi^2$/dof |
|---|---|---|---|---|---|---|---|---|---|---|---|
| 0–5 | 0.800 | 0.887 | -2.050 | 2.900 | 4.819 | 4.500 | 7.500 | 100 | 119 | 308 | 7.551 / 32 |
| 5–10 | 0.779 | 0.886 | -2.090 | 3.005 | 4.591 | 5.000 | 7.994 | 75 | 104 | 248 | 7.967 / 33 |
| 10–20 | 0.767 | 0.876 | -2.100 | 3.100 | 4.500 | 5.100 | 8.750 | 53 | 80 | 236 | 4.447 / 33 |
| 20–40 | 0.743 | 0.818 | -2.300 | 3.300 | 4.353 | 5.150 | 8.900 | 32 | 47 | 200 | 1.461 / 32 |
| 40–60 | 0.713 | 0.817 | -2.750 | 4.500 | 4.350 | 6.000 | 9.500 | 18 | 31 | 157 | 0.693 / 33 |
| 60–80 | 0.660 | 0.563 | -2.760 | 4.700 | 4.200 | 6.500 | 10.000 | 9 | 18 | 95 | 0.463 / 33 |
| 80–100 | 0.608 | 0.129 | -2.800 | 4.710 | 4.101 | 6.998 | 10.050 | 4 | 9 | 31 | 0.137 / 32 |

- The midrapidity gluon-gluon source is the largest hadron production source at all centralities, the *p*-like source the smallest
- The width $\Gamma_{gg}$ increases towards more peripheral collisions

Calculations: P. Schulz and GW (2014)
From $\chi^2$- minimizations with respect to the prel. ALICE data.

Preliminary data: A. Toia (ALICE collab./ CL1), Nucl. Phys. A931, 315 (2014)

# Conclusion Particle production sources

- Charged-hadron production at RHIC and LHC energies has been investigated in a Relativistic Diffusion Model (RDM).

- Predictions of pseudorapidity distributions $dN/d\eta$ of produced charged hadrons in the 3-sources RDM at LHC energies, and comparisons with ALICE data have been performed.

- The contribution of the fragmentation sources from quark-gluon collisions at LHC energies is substantial at larger values of pseudorapidity $\eta$.

- Between RHIC and LHC energies, the midrapidity gluon-gluon source becomes more important than the fragmentation sources. The total particle content in this source rises with $\ln^3(\sqrt{s_{NN}})$.

- Charged-hadron production in pPb @ 5.02 TeV and its centrality dependence is well reproduced. The midrapidity source dominates at all centralities.

# 4. Upsilon Suppression in PbPb @ LHC

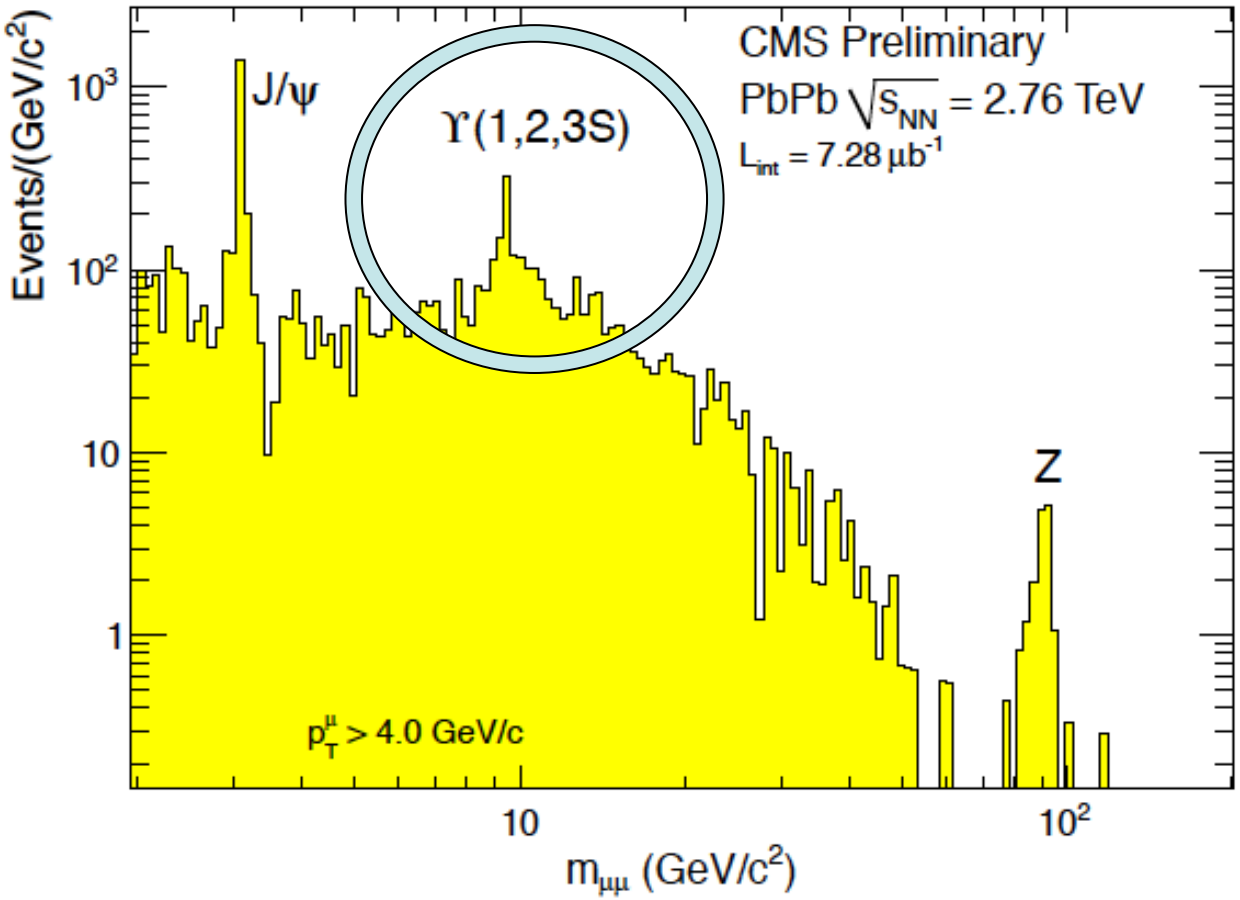


ϒ suppression as a sensitive probe for the QGP

- No significant effect of regeneration
- $m_b \approx 3m_c$ ⇨ cleaner theoretical treatment
- More stable than J/ψ

$E_B(\Upsilon_{1S}) \approx 1.10$ GeV
$E_B(J/\psi) \approx 0.64$ GeV

**CMS Collab., CMS-PAS-HIN-10-006 (2011)**

# Υ(nS) states are suppressed in PbPb @ LHC:

CMS

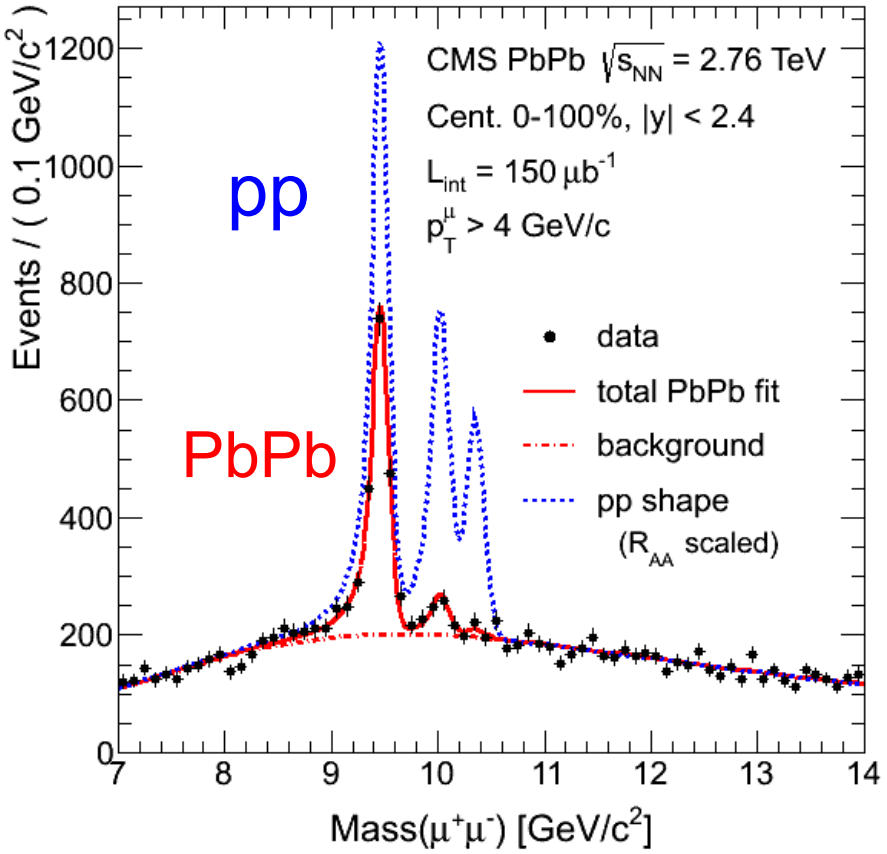


$$R_{AA} = \frac{N_{PbPb}(Q\bar{Q})}{N_{coll} N_{pp}(Q\bar{Q})}$$

## A clear QGP indicator

1. Υ(1S) ground state is suppressed in PbPb:

$R_{AA}$ (Υ(1S)) = 0.56 ± 0.08 ± 0.07 in min. bias

2. Υ(2S, 3S) states are > 4 times stronger suppressed in PbPb than Υ(1S)

$R_{AA}$(Υ(2S)) = 0.12 ± 0.04 (stat.) ± 0.02 (syst.)

$R_{AA}$(Υ(3S)) = 0.03 ± 0.04 (stat.) ± 0.01 (syst.)

**CMS Collab., PRL 109, 222301 (2012)**
**[Plot from CMS database]**

# Screening, Gluodissociation and Collisional broadening of the Υ(nS) states

- Debye screening of all states involved: Static suppression
- The imaginary part of the potential (effect of collisions) contributes to the broadening of the Υ(nS) states: damping
- Gluon-induced dissociation: dynamic suppression, in particular of the Υ(1S) ground state due to the large thermal gluon density
- Reduced feed-down from the excited $\Upsilon/\chi_b$ states to Υ(1S) substantially modifies the populations: indirect suppression

**F. Vaccaro, F. Nendzig and GW, Europhys.Lett. 102, 42001 (2013); J. Hoelck and GW, unpublished**
**F. Nendzig and GW, Phys. Rev. C 87, 024911 (2013); J. Phys. G41, 095003 (2014)**
**F. Brezinski and GW, Phys. Lett.B 70, 534 (2012)**

# Screening and damping treated in a nonrelativistic potential model

$$V_{nl}(r,T) = -\frac{\sigma}{m_D(T)} e^{-m_D(T)r} - C_F \alpha_{nl}(T) \left( \frac{e^{-m_D(T)r}}{r} + iT\phi(m_D(T)r) \right)$$

$$\phi(x) = \int_0^\infty \frac{dz\, 2z}{(1+z^2)^2} \left( 1 - \frac{\sin xz}{xz} \right), m_D(T) = T\sqrt{4\pi\alpha_s(2\pi T)\frac{2N_c + N_f}{6}}$$

From the literature

Screened potential: $m_D$ = Debye mass,
$\alpha_{nl}(T)$ the strong coupling constant;
$C_F = (N_c^2 - 1) / (2N_c)$
$\sigma \approx 0.192$ the string tension (Jacobs et al.; Karsch et al.)

Imaginary part: Collisional damping (Laine et al. 2007, Beraudo et al. 2008, Brambilla et al. 2008) for $2\pi T >>$ <1/r>; different form for $2\pi T <<$ <1/r>.

# Screening and damping

Constrain Re$V_s(r)$ by lattice QCD data on the singlet free energy

*Maximal value*

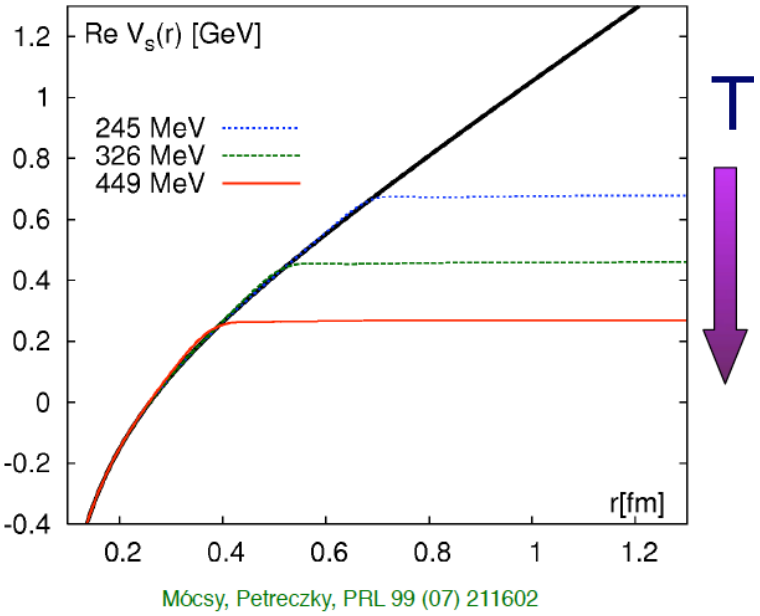


Mócsy, Petreczky, PRL 99 (07) 211602

T

Take Im$V_s(r)$ from pQCD calculations

*Minimal value*

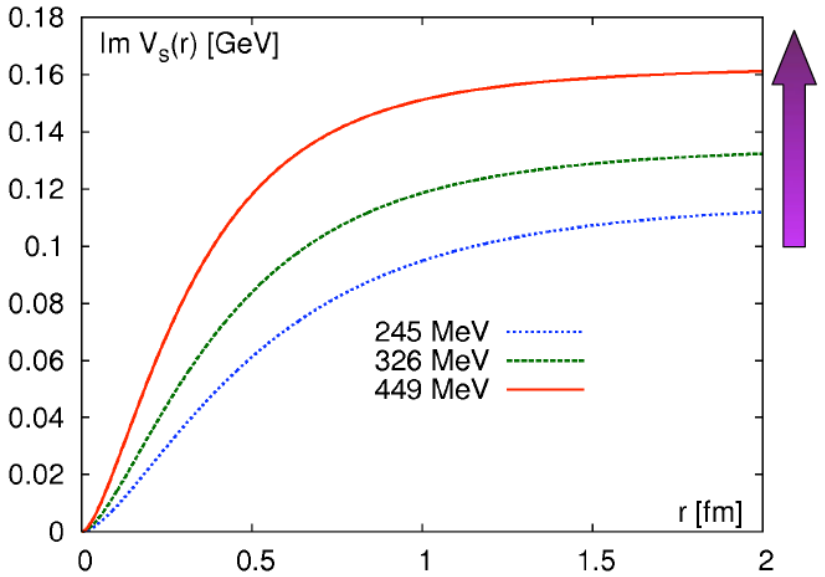


Burnier, Laine, Vepsalainen JHEP 0801 (08) 043
Beraudo, arXiv:0812.1130

From: A. Mocsy et al.

Screening

Damping

# Radial wave function of Υ(1S)

Solutions of the Schoedinger equation with complex potential V(r,T,$\alpha_s$) for the radial wave functions $g_{nl}$(r,T),

$$[H(r,T,\alpha_s) - E + i\Gamma/2]g(r) = 0$$

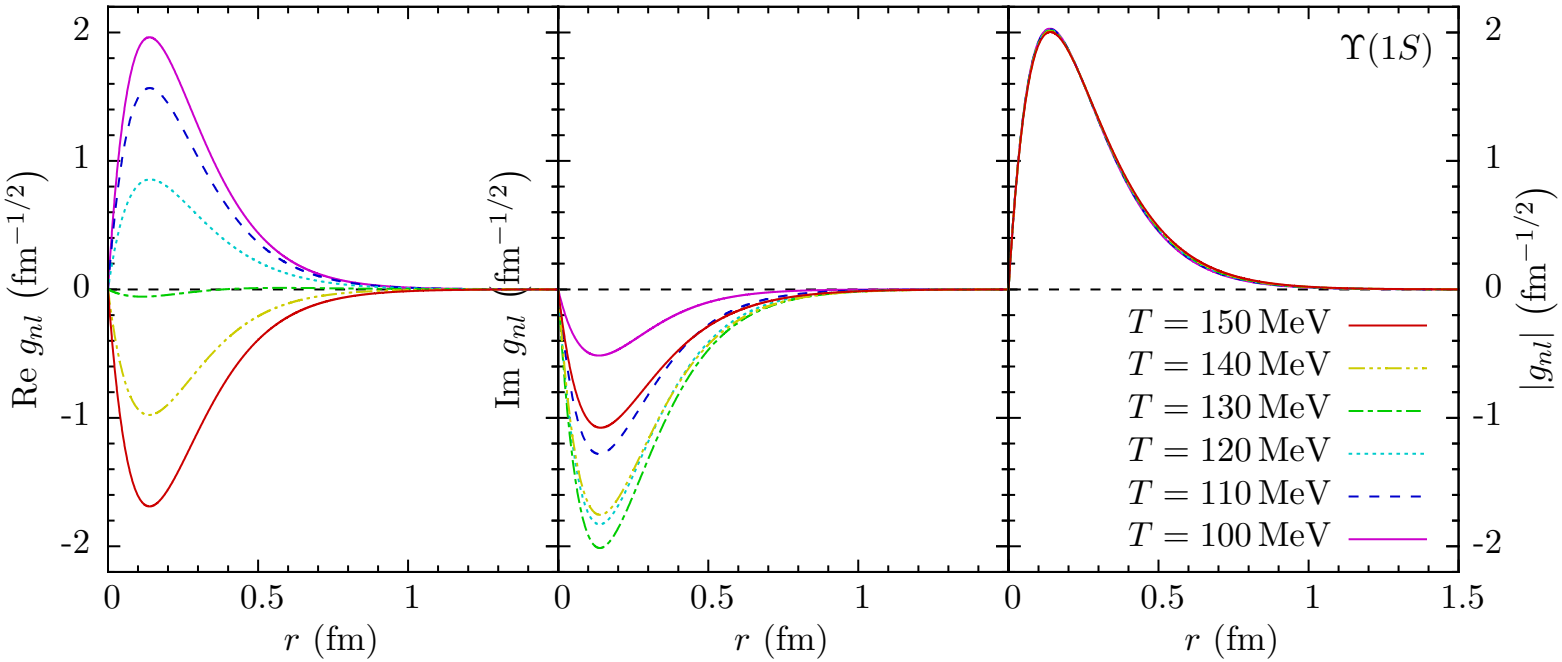


From: J. Hoelck and GW, unpublished

# Cross section for gluodissociation

Born amplitude for the interaction of gluon clusters according to Bhanot&Peskin in dipole approximation / Operator product expansion, extended to include the screened coulombic + string eigenfunctions as outlined in Brezinski and Wolschin, PLB 70, 534 (2012)

$$\sigma_{diss}^{nS}(E) = \frac{2\pi^2 \alpha_s E}{9} \int_0^\infty dk\, \delta\left(\frac{k^2}{m_b} + \epsilon_n - E\right) |w^{nS}(k)|^2$$

$$w^{nS}(k) = \int_0^\infty dr\, r\, g_{n0}^s(r) g_{k1}^a(r)$$

for the Gluodissociation cross section of the Y(nS) states, and correspondingly for the $\chi_b$(nP) states.

# Gluodissociation cross section

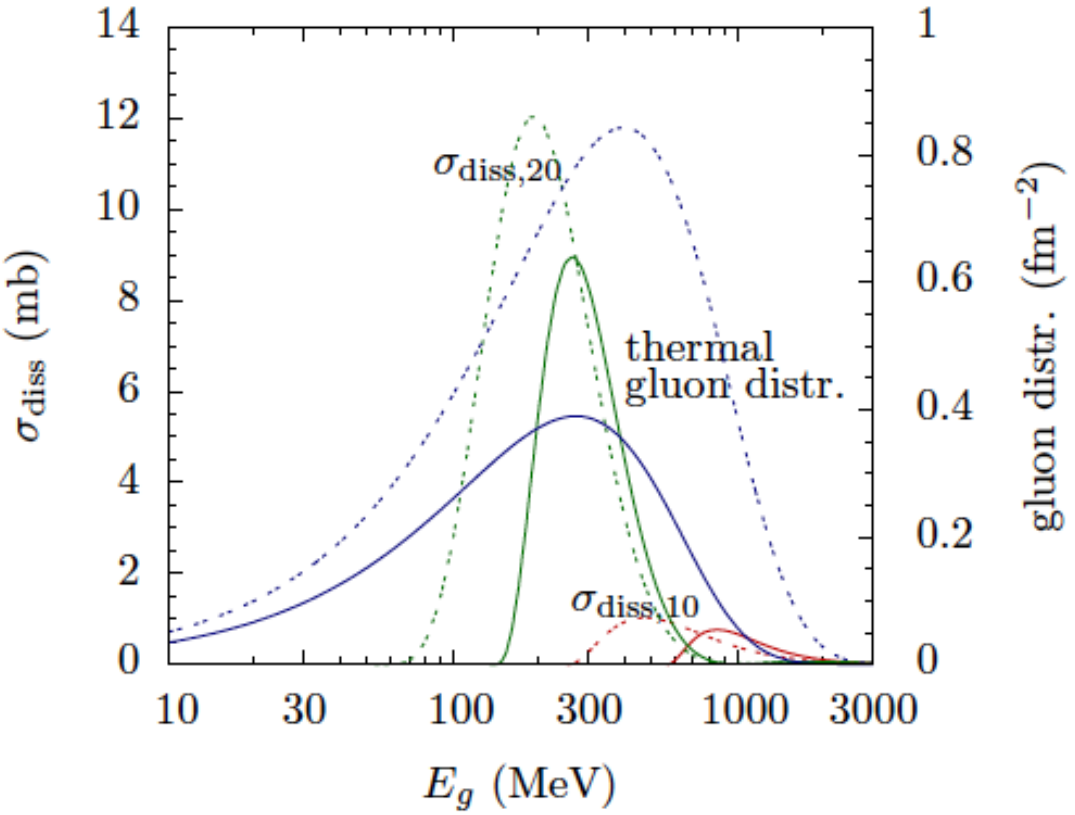


**Figure 3.** Gluodissociation cross section $\sigma_{diss}$ (left scale) of the $\Upsilon(1S)$ and $\Upsilon(2S)$ and the thermal gluon distribution (right scale) plotted for temperature $T = 170$ (solid curves) and 250 MeV (dotted curves) as functions of the gluon energy $E_g$.

F. Nendzig and GW, J. Phys. G41, 095003 (2014)

# Dynamical fireball evolution

Dependence of the local temperature T on impact parameter b, time t, and transverse coordinates x, y evaluated in ideal hydrodynamic calculation with transverse expansion

$$T(b, \tau_{init}, x^1, x^2) = T_0 \left( \frac{N_{mix}(b, x^1, x^2)}{N_{mix}(0,0,0)} \right)^{1/3}$$

$$N_{mix} = \frac{1-f}{2} N_{part} + f N_{coll}, \qquad f = 0.145$$

The number of produced $b\bar{b}$-pairs is proportional to the number of binary collision, and the nuclear overlap

$$N_{b\bar{b}}(b,x,y) \propto N_{\rm coll}(b,x,y) \propto T_{AA}(b,x,y)$$

QGP suppression factor (without feed-down and CNM effects):

$$R_{AA}^{QGP} = \frac{\int d^2b \int dxdy\, T_{AA}(b,x,y)\, e^{-\int_{t_F}^{\infty} dt\, \Gamma_{\rm tot}(b,t,x,y)}}{\int d^2b \int dxdy\, T_{AA}(b,x,y)}$$

# Feed-down cascade including $\chi_{nP}$ states

Relative initial populations in pp computed using an inverted cascade from the final populations measured by CMS and CDF($\chi_b$)
[$N_{final}(1S):=1$]

$N_{initial}$

3S: 0.387

2S: 0.371

1S: 0.458

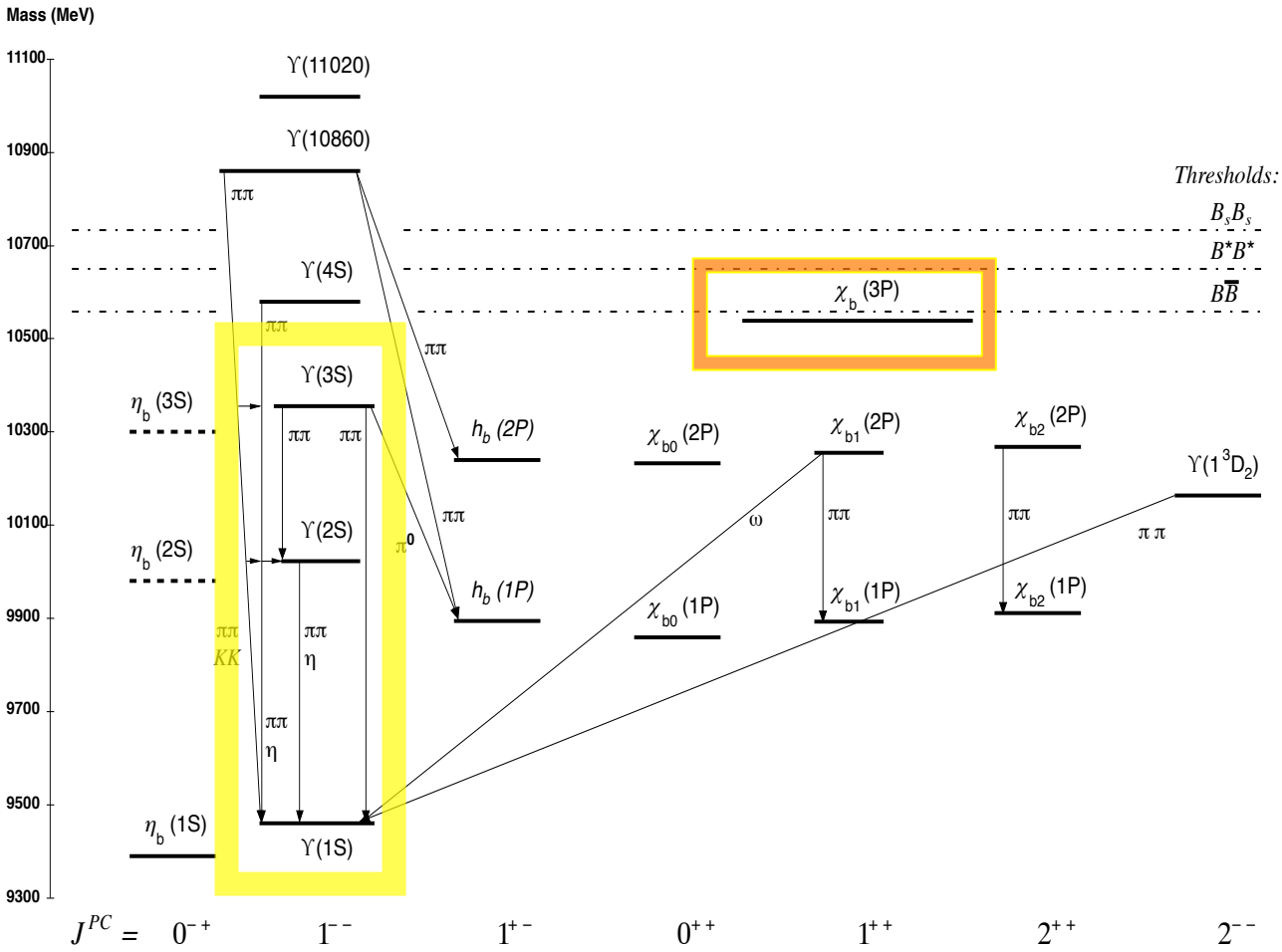


$N_{initial}$

2P: 0.976

1P: 1.29

# Theoretical vs. exp. (CMS) Suppression factors

- Screening (potential model)
- Collisional damping (imaginary part of potential)
- Gluodissociation (OPE with string tension included)
- Reduced feed-down from excited states

$t_F$: Y formation time
$t_{QGP}$: QGP lifetime
$T_{max}$ @ $t_F$: 200-800 MeV

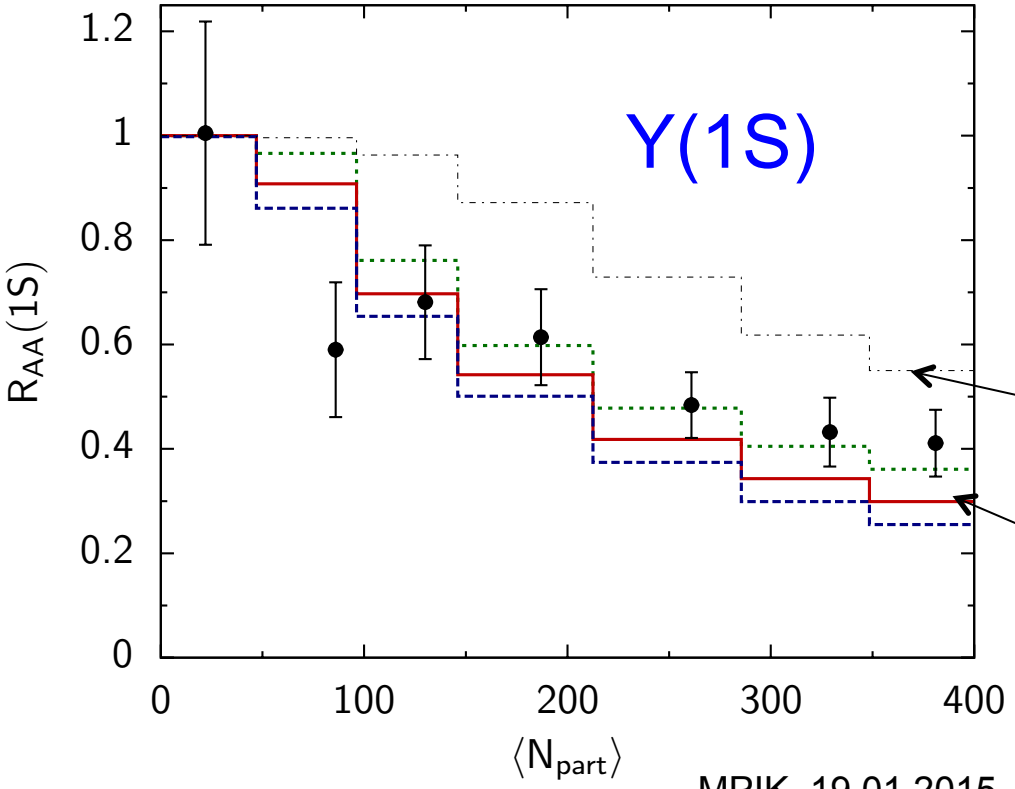


$t_F$= 0.1 fm/c
$t_{QGP}$= 4, 6, 8 fm/c

QGP suppression

with modified feed-down cascade

**F. Nendzig and GW, Phys. Rev. C 87, 024911 (2013)**

MPIK_19.01.2015

# Theoretical vs. exp. (CMS) Suppression factors

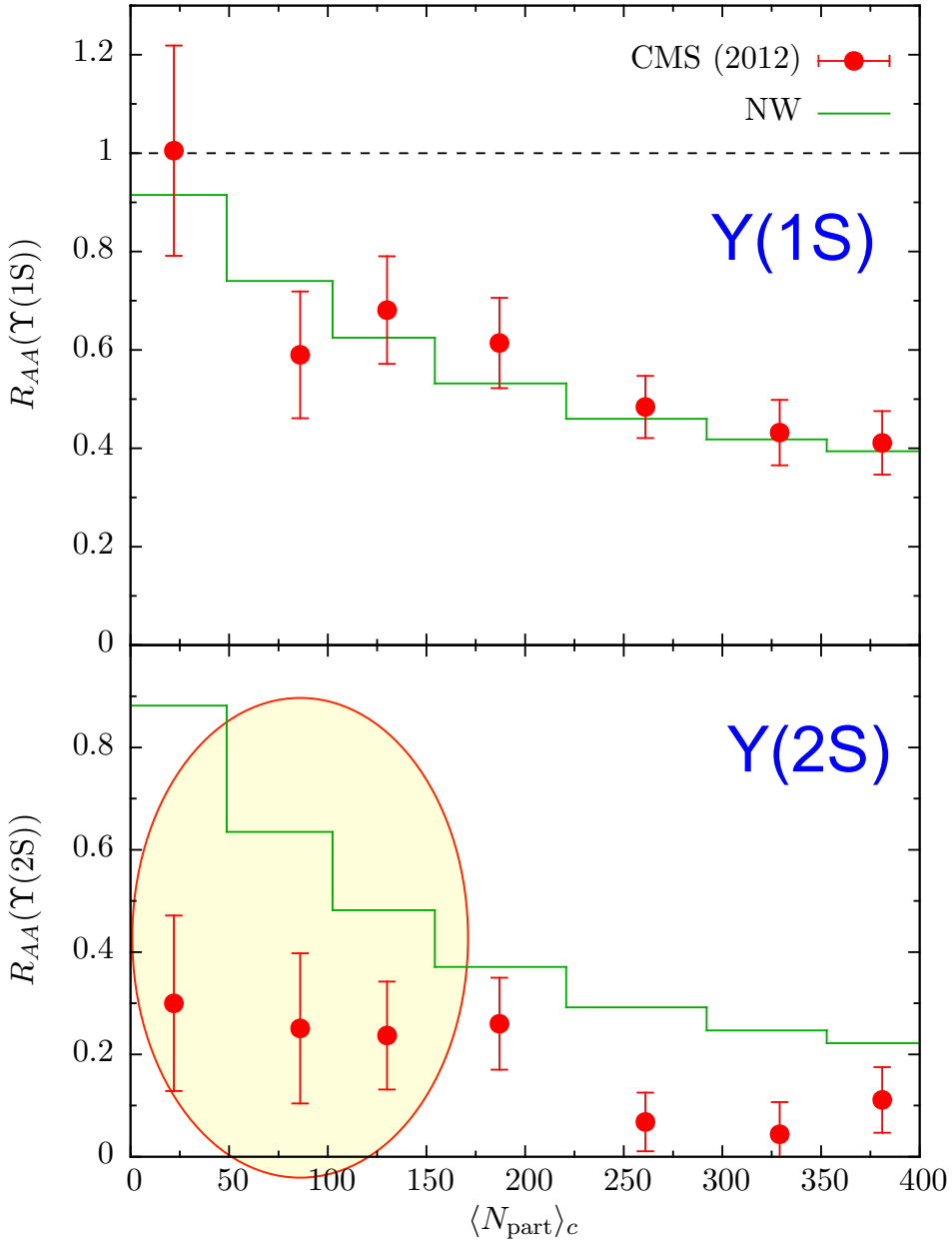


2014: Substantial improvements of the model

- Consider running of the coupling
- Transverse momentum of the Y included
- Relativistic Doppler effect
- Improved initial conditions
- $T_c$ = 160 MeV

$t_F$= 0.4 fm/c: Y formation time
$T_{max}$= 550 MeV: central temp. at b = 0 and t = $t_F$

Room for additional suppression mechanisms for the excited states: Hadronic dissociation, mostly by pions, is one possibility. Thermal pions are insufficient; direct pions may contribute.

**F. Nendzig and GW, J. Phys. G41, 095003 (2014); J. Hoelck and GW, unpublished**

# Prediction for Υ(1S) suppression at 5.125 TeV

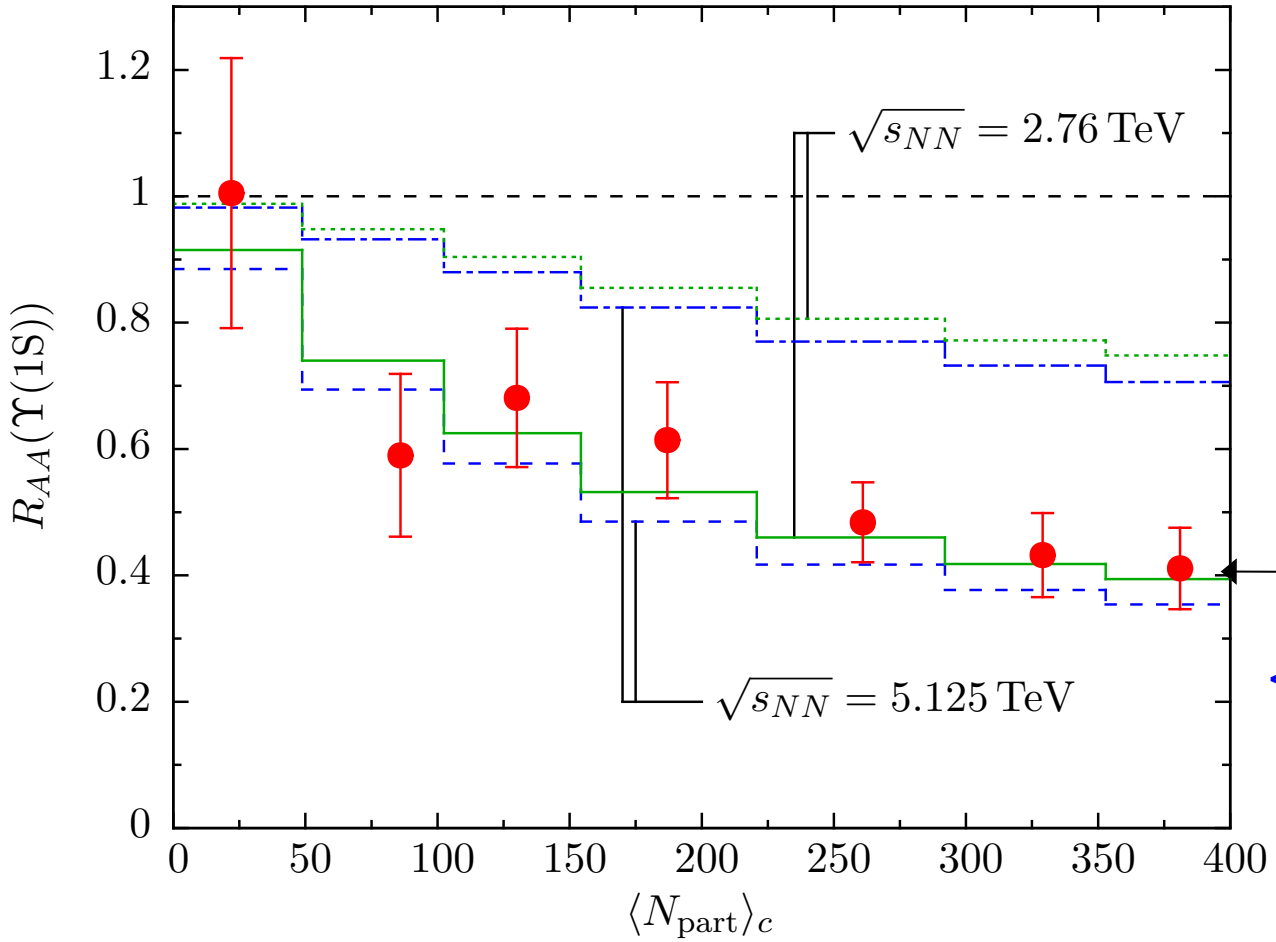


$t_F$: Y formation time
$T_{max}$ @ $t_F$: 579 MeV

$t_F$= 0.4 fm/c; use

$$s_0 \propto dN_{ch}/d\eta \propto T_0^3$$

with reduced feed-down

<10% more suppression at 5.125 TeV vs 2.76 TeV

**F. Hoelck and GW, unpublished**

# Conclusion Upsilon suppression

- The suppression of the $\Upsilon$(1S) ground state in PbPb collisions at LHC energies through gluodissociation, damping, screening, and reduced feed-down has been calculated for min. bias, and as function of centrality, and is found to be in good agreement with the CMS result. Screening is not decisive for the 1S state except for central collisions.

- The enhanced suppression of the $\Upsilon$(2S, 3S) relative to the 1S state in PbPb as compared to pp collisions at LHC energies (CMS) leaves room for additional suppression mechanisms, in particular for peripheral collisions where discrepancies to the CMS data persist. Hadronic and/or magnetic dissociation of the excited states may be relevant.

Thank you for your attention !